Distance Protection of AC Grid With HVDC-Connected Offshore Wind Generators

Lina He, *Student Member, IEEE*, Chen-Ching Liu, *Fellow, IEEE*, Andrea Pitto, *Member, IEEE*, and Diego Cirio, *Senior Member, IEEE*

***Abstract*—When a transmission line close to points of common coupling (PCCs) experiences a short-circuit (SC) fault, the fast reactive power control of voltage-source converter-HVDC (VSC-HVDC) is likely to affect the protective relay operation of transmission lines. To study the performance of distance relays on an ac grid with an offshore wind HVDC network, this paper presents an apparent impedance calculation method, which utilizes the bus impedance matrix (Zbus) to calculate the impedances viewed by distance relays during a three-phase SC fault. The proposed method is used to identify the potential miscoordinated Zone 2 relays in the proposed combined ac/dc system. The analysis is verified by software simulation results. It is shown that the proposed method results in accurate impedances viewed by distance relays. It also identifies the protective device settings on the ac grid that need to be adjusted due to HVDC control of offshore wind generators.**

***Index Terms*—Decoupling control of VSC, distance relays, offshore wind farms, VSC-HVDC, Zbus.**

I. Introduction

WITH the increasing energy demand and growing environmental concern, many countries have developed their targets to significantly increase the integration of renewable energy sources, including offshore wind power. A report from European Wind Energy Association (EWEA) has shown that the installation capacity of EU offshore wind units will be increased to 40–50 GW in 2020 from 2 GW in 2009 [1]. The rapid growth of offshore wind power and its inherent characteristics (e.g., large scale and long distances) make the integration of offshore wind power to onshore grids a great technical challenge. It is shown in existing studies that VSC-HVDC is preferred for offshore wind power transmission due to its advantages of fast and independent control of active and reactive power, feasibility of multi-terminal dc grids, and black start capability [2], [3].

Manuscript received February 21, 2012; accepted June 17, 2013. Date of publication July 18, 2013; date of current version March 20, 2014. This work was supported by the EU project Transmission system operation with large penetration of wind and other renewable electricity sources in networks by means of innovative tools and integrated energy solutions (TWENTIES). Paper no. TPWRD-00179-2012.

L. He is with the University College Dublin, Belfield, Dublin 4, Ireland (e-mail: lina.he@ucdconnect.ie).

C.-C. Liu is with the Washington State University, Pullman, WA 99164-2752 USA and also with University College Dublin, Belfield, Dublin 4, Ireland (e-mail: liu@ucd.ie).

D. Cirio and A. Pitto are with the RSE – Ricerca sul Sistema Energetico S.p.A., Milan 20134, Italy (e-mail: diego.cirio@rse-web.it; andrea.pitto@rse-web.it).

Digital Object Identifier 10.1109/TPWRD.2013.2271761

In an offshore wind HVDC network, the main task of HVDC link is to collect offshore wind power and deliver it to the ac grid. Generally, the grid side VSC (GSVSC) uses the constant dc and ac voltage control mode to independently regulate the transmitted active and reactive power. When an ac transmission line close to a PCC undergoes a SC fault, there are technical requirements for the dc side protection [4]. In such a case, the PCC voltage is reduced, which in turn affects voltages and currents of ac transmission grid close to the PCC. Since the capacity of VSC stations is generally large for the offshore power transmission, their impact on the line voltages and currents will be significant. It is likely to significantly impact the performance of existing protection schemes on the ac grid, such as distance protections. The basic principle of distance relaying is to measure the apparent impedance using the voltage and current viewed by a relay, which approximately determines the distance between the relay location and fault point during a SC fault. The apparent impedance is compared with pre-set relay operation characteristics to decide whether the fault is within the protected zone. Appropriate time delays are used to allow primary and back-up functions among the distance relays.

The Zone 2 relay is a back up protective function that is usually located on the remote end of a line adjacent to the protected line [5]. Due to the impact of VSC fast control (in the order of milliseconds) on line voltages and currents, impedances viewed by Zone 2 relays might fail to locate the fault in case of a SC fault on lines emanating from the remote bus. The error in the fault distance location will result in miscoordination, e.g., a Zone 2 fault is not cleared at the expected time delay. If the fault clearing time exceeds the critical clearing time (CCT), the system can suffer instability and potentially trigger a sequence of cascading events [6].

Studies have been conducted on the effect of flexible alternating current transmission (FACTS) devices on distance relays on an ac grid [7]–[9]. Most of FACTS devices are based on the full-controlled electronic switch technology that allows devices to fast regulate reactive power exchange with the ac grid. The study in [7] evaluates the performance of distance relays on transmission lines compensated by shunt FACTS, including static var compensators (SVC) and static synchronous compensator (STATCOM). The work of [8] reports the effect of unified power flow controllers (UPFCs) on distance relays under different fault conditions using an apparent impedance calculation method based on sequence components. Reference [9] provides an analysis of the tripping boundary of a distance relay on a transmission line equipped with UPFC, which is mainly related to the location and control parameters of a UPFC. In addition,

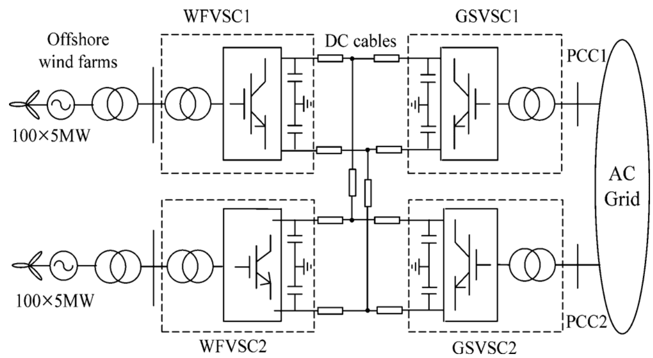

Fig. 1. AC/DC system.

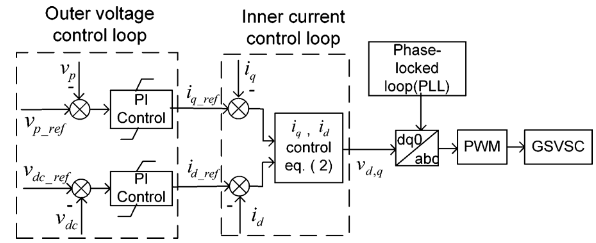

Fig. 2. Simplified control configuration of GSVSCs.

the work of [10] analyzes the performance of a distance relay of a transmission line connected to a wind farm with different conditions. Reference [11] discusses a Zone 2 setting calculation method, which is based on software simulations of faults on the reach of Zone 1 with the maximum and minimum generation of an ac grid. To the best of the authors' knowledge, the existing research does not involve the performance of distance relays on an ac grid with HVDC-connected offshore wind generators.

With the growing penetration of offshore wind power, an increasing number of VSC stations will be set up for the integration of offshore wind power. The impact of GSVSCs reactive control on distance relays on ac grids has become an important subject. The issue of miscoordination of Zone 2 protection caused by HVDC control needs to be addressed. This paper proposes an apparent impedance calculation method for identification of potential miscoordinated relays. By considering GSVSCs reactive power regulation, the proposed method uses Zbus method to calculate impedances viewed by distance relays. It is applied to the proposed combined ac/dc system to calculate the impedance viewed by a distance relay during a SC fault at the reach of its Zone 2. The calculation results are compared with the corresponding Zone 2 settings to identify miscoordinated relays. The proposed method can be used by protection/planning engineers to identify protective device settings that need to be adjusted due to HVDC control.

The organization of this paper is as follows. Section II outlines an offshore wind HVDC network and the corresponding HVDC control. The proposed apparent impedance calculation method is discussed in Section III. It is applied to all distance relays on the proposed combined ac/dc system. The potential miscoordinated relays and the level of impact of offshore wind HVDC network on distance relays are reported in Section IV. The results are compared with software simulation results to validate the accuracy of the proposed method. Section V concludes.

II. System Outline

A. An Overview

Fig. 1 illustrates an example of multi-terminal HVDC grid for the integration of offshore wind farms: two 500 MW offshore wind farms based on Doubly Fed Induction Generators (DFIGs) are connected to an ac grid via an H-shaped VSC-HVDC grid in the bipolar configuration which is interfaced to ac systems through four VSCs, i.e., two wind farm side VSCs (WFVSCs) and two GSVSCs.

B. VSC-HVDC Control

In a VSC-HVDC link, a constant dc voltage can automatically balance the sent and received active power. It does not require any communication between WFVSCs and GSVSCs. WFVSCs usually control the magnitude and the frequency of the offshore ac side voltage to enable the collection of all offshore wind power [2]. GSVSCs are assigned to control the voltage of the dc grid. The power-voltage droop control mode is used to coordinate dc voltage control of GSVSCs. In addition, GSVSCs provide reactive power support for the ac grid to maintain PCC voltages at an expected level. In the proposed ac/dc system, shown in Fig. 1, two GSVSCs use the same control mode and parameters.

The GSVSC control configuration is shown in Fig. 2. It consists of the outer voltage and inner current control loops. The outer voltage control loop is to regulate the GSVSC dc side voltage $(v_{\rm dc})$ and PCC voltage (v_p) by PI controllers with their corresponding reference values $v_{\rm dc\_ref}$ and $v_{p\_\rm ref}$. The reference value of the GSVSC dc side voltage is obtained by the power-voltage droop control

$$v_{\rm dc\_ref} = v_{\rm dc} + k(P - P_{\rm ref}) \tag{1}$$

where P is the active power transmitted by GSVSC, the subscript "_ref" means the reference value and the symbol k is the slope of the voltage-power droop characteristic curve. The inner current control loop uses a feed-forward current decoupling controller to achieve independent control of active and reactive power. The corresponding control equations are given as follows [2]:

$$\begin{aligned} v_d &= \left(k_{iP} + \frac{k_{iI}}{s}\right)(i_{d\_\rm ref} - i_d) - \omega L i_q + v_{p\_d} \\ v_q &= \left(k_{iP} + \frac{k_{iI}}{s}\right)(i_{q\_\rm ref} - i_q) + \omega L i_d + v_{p\_q} \end{aligned} \tag{2}$$

where $v(i)_d$ and $v(i)_q$ are d, q axis components of GSVSC ac side voltage (current), respectively. The symbols k_{ip} and k_{il} represent the proportional and integral gains of the PI current controller. The voltages v_{p_d} and v_{p_q} are d, q axis components of the PCC voltage. The symbols ω and L correspond to the angular speed of the synchronous d-q frame and GSVSC commutation reactance, respectively. The symbol s is the differential operator with respect to time.

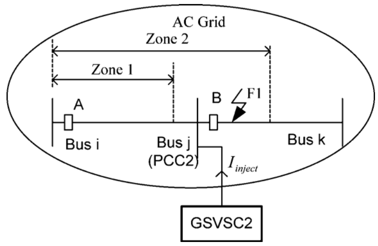

Fig. 3. Portion of proposed system.

C. Distance Protection of AC Grid

Offshore wind farms are expected to be connected into transmission levels of ac grids due to their large capacity. In ac transmission systems, distance relaying is commonly designed with primary and backup protection. Its operation characteristics are predefined with fixed settings based on detailed offline system studies. Distance relays are arranged to provide two or three protective zones for transmission lines. Zone 1 is set to protect 80%-90% of the line length and operate with no intentional time delay. Due to the inherent time delay of protective devices, such as measurement and sampling devices, the operation time of Zone 1 relay is typically 2 cycles. As a backup protection, Zone 2 is required to reach 40%-50% of the shortest line emanating from the remote bus with an appropriate time delay (typically 15–30 cycles) [5], [12]. The reach of Zone 3 exceeds the adjacent line and its typical time delay is 1 s [5]. Fixed time delays help to coordinate different zones of distance relays.

For this study, it is assumed that transmission lines of the ac grid with offshore wind HVDC network are protected by distance relays. Zone 2 is set to reach 50% of the shortest line emanating from the remote bus with 20 cycles time delay. Considering the operation time of relays (2 cycles), the fault clearing time of Zone 2 is about 22 cycles in the event of a Zone 1 failure.

D. Discussion of Impact of GSVSC Control on Distance Relays

Fig. 3 shows a portion of the proposed ac/dc system, which is used to discuss the impact of GSVSC control on distance relays. When line j-k experiences a SC fault F1, the reduction of bus j voltage triggers GSVSC2 to increase reactive power output to boost PCC2 voltage. Since relay B and fault F1 are located in the same transmission line, the reactive power control does not affect the impedance viewed by relay B. Assuming the fault impedance is 0, the impedance viewed by relay B corresponds to the line impedance from the fault point to relay location.

Fault F1 is in the range of Zone 1 of relay B and Zone 2 of relay A. If the primary protection (Zone 1 of relay B) fails to clear fault F1, relay A will work as the backup protection to clear the fault with Zone 2 time delay. The duration allows the fast adjustment of GSVSC2 reactive power. Bus j voltage is increased, leading to an increased bus i voltage and reduced line i-j current. As a result, the impedance viewed by relay A is increased and the fault distance viewed by relay A is overestimated.

It is found that the fault distance viewed by a relay is overestimated when a reactive power source is located between the fault point and relay location. A Zone 2 fault is likely to be viewed as a Zone 3 event. As a result, the Zone 2 fault is cleared with the Zone 3 time delay. The longer fault clearing time reduces the margin of system stability, endangering system security under severe conditions.

III. Apparent Impedance Calculation Method in an AC/DC System

To find potential miscoordinated Zone 2 relays in an ac grid with offshore wind HVDC network, an apparent impedance calculation method based on Zbus is presented in this paper. The calculation procedure consists of three steps:

(1) Calculate PCC voltages based on Zbus method during a three-phase SC fault located on 50% of the shortest line emanating from the remote bus of a relay;
(2) Consider GSVSCs reactive power control to modify PCC voltages;
(3) Use Zbus method to calculate the voltage and current viewed by the relay based on PCC voltages obtained in step (2), and compare the obtained apparent impedance with the Zone 2 setting of the relay.

A. Estimation of PCC Voltages During Fault Based on Zbus

The Zbus approach is used to calculate nodal voltages and the fault currents during a three-phase SC fault [6]. Since GSVSCs use the constant ac voltage control mode, the PCC voltage will be maintained at the nominal value under a normal condition. In the calculation, GSVSC can be modeled as a constant voltage source, which is connected to the corresponding PCC. Reactance of the commutating reactor of GSVSC is seen as the reactance of the equivalent voltage source.

Fig. 4 shows a case about the Zone 2 setting evaluation of relay S. Assuming line n-r is the shortest line emanating from the remote bus n, the three-phase SC fault k is located at 50% of line n-r. The voltage at bus p, i.e., PCC voltage, is given by

$$V_p = V_p^0 - \frac{Z_{pk}}{Z_{kk}} V_k^0,\ p \in \mathrm{L} \tag{3}$$

where L is the set of all PCCs, V_p^0 and V_k^0 are referred to the pre-fault voltages of bus p and fault point k, respectively. V_k^0 can be represented as [12], [13]

$$V_k^0 = 0.5V_n^0 + 0.5V_r^0 \tag{4}$$

where V_n^0 and V_r^0 correspond to pre-fault voltages of bus n and bus r, respectively. The transfer impedance between bus p and fault point k (Z_{pk}) and the driving point impedance corresponding to fault point k (Z_{kk}) are given by [12], [13]

$$Z_{pk} = 0.5Z_{pn} + 0.5Z_{pr} \tag{5}$$
$$Z_{kk} = 0.25Z_{nn} + 0.25Z_{rr} + 0.5Z_{nr} + 0.25Z_{n-r} \tag{6}$$

where $Z_{pn(r)}$ is the transfer impedance between bus p and bus n(r), Z_{nn} and Z_{rr} are the driving point impedance corresponding to bus n and bus r, respectively, Z_{nr} is the transfer impedance between buses n and r, and Z_{n-r} denotes the impedance of line n-r.

The proposed method is to estimate PCC voltages at the instant of Zone 2 tripping. The Zone 2 fault clearing time is set to

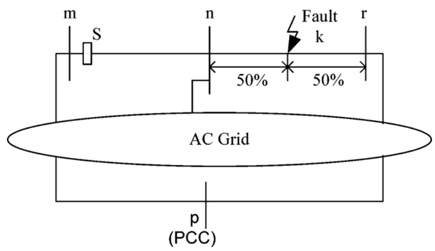

Fig. 4. Case of Zone 2 setting evaluation of relay S.

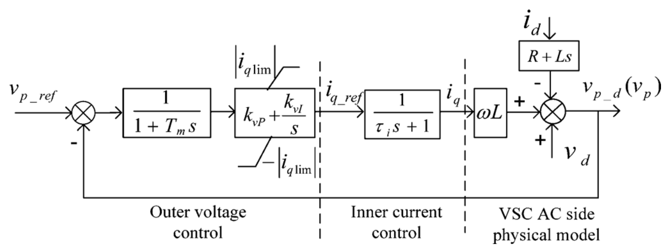

Fig. 5. PCC voltage control loop of GSVSCs.

22 cycles, e.g., 0.37 s in a 60 Hz ac grid. In ac grids, the subtransient open circuit time constant of a synchronous generator is in the range of 0.01–0.05 s, and the transient open circuit time constant lies between 1.5 and 10 s [6]. The transient impedances of generators are used to construct Zbus in the proposed method. It makes the estimated PCC voltages close to actual PCC voltages at the Zone 2 fault clearing time. The obtained PCC voltages are the initial value of PCC voltages at the transient state.

B. Change in PCC Voltage Estimation by Considering GSVSC Reactive Power Control

The GSVSC control configuration is shown in Fig. 2. Due to coupling of HVDC model in d, q frame, the inner current controller is used to achieve decoupling of the d, q axis models. The PCC voltage control loop of a GSVSC can be represented as Fig. 5.

In Fig. 5, v_{p_ref} is the reference value of a PCC voltage; $1/(1+T_m s)$ is the inertia block of the voltage sampling and measurement, where T_m is the corresponding time constant and its typical value is 0.01 s [14]; $k_{vP}+k_{vI}/s$ is the PI voltage controller, where k_{vP} and k_{vI} refer to the proportional and integral gains of the voltage controller, respectively. The symbol $i_{q\,\lim}$ corresponds to the limit value of the q-axis component of the VSC ac side current. Compared with the outer voltage control, the inner current control demonstrates a faster dynamic response during a disturbance due to the high switching frequency (generally over 1 kHz). Hence, inner current control is represented as an inertia block $1/(\tau_i s+1)$. The time constant τ_i is typically in the range of 0.5–3 ms [14]. In the d, q decoupling control, the ac side voltage phasor of the GSVSC is chosen as the d-axis reference phasor, i.e., the d-axis component of PCC voltage v_{p_d} is the PCC voltage v_p. The GSVSC ac side physical model in d-axis is based on

$$v_{p\_d} = -L\frac{di_d}{dt} - Ri_d + \omega L i_q + v_d \tag{7}$$

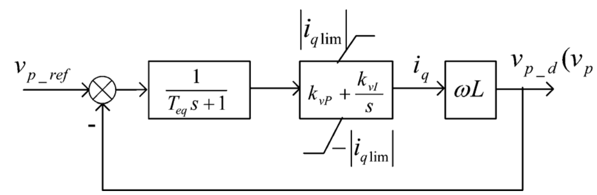

Fig. 6. Simplified PCC voltage control loop of GSVSCs.

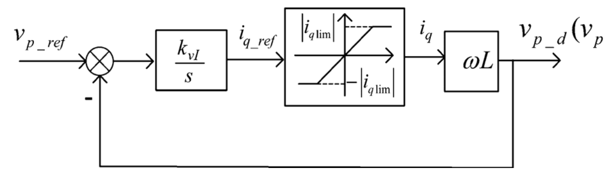

Fig. 7. Simplified PCC voltage control loop of GSVSCs.

where R, L and ω are the resistance and inductance of the commutating reactor, and the ac grid frequency, respectively.

Since $\tau_i << T_m << 1$, two inertia blocks can be combined and the equivalent time constant T_{eq} is $T_m + \tau_i$. To study dynamics of the PCC voltage, it is reasonable to ignore the impact of disturbance variables, i_d and v_d. The simplified control loop of PCC voltage is represented in Fig. 6.

The open loop transfer function of PCC voltage is given by

$$\begin{aligned} W_o(s) &= \frac{1}{1+T_{eq}s} * \frac{k_{vP}s + k_{vI}}{s} * \omega L \\ &= \frac{\omega L k_{vI}(\frac{k_{vP}}{k_{vI}}s+1)}{(1+T_{eq}s)s} \end{aligned} \tag{8}$$

which is an integral-type system. To obtain a fast response in the control system, the compensator zero $s = -k_{vI}/k_{vP}$ is designed to cancel the plant pole $s = -1/T_{eq}$. Thus, the open loop transfer function can be simplified to

$$W_o'(s) = \frac{\omega L k_{vI}}{s}. \tag{9}$$

The simplified control loop is shown in Fig. 7. The PCC voltage is governed by the following dynamic model:

$$\frac{dv_p}{dt} + \omega L k_{vI} v_p = \omega L k_{vI} v_{p\_\mathrm{ref}}. \tag{10}$$

Considering the PCC voltage V_p obtained in Section III-A as the initial value with HVDC control during fault k, the solution of (10) is given by

$$v_p(t) = (V_p - v_{p\_\mathrm{ref}})e^{-\omega L k_{vI} t} + v_{p\_\mathrm{ref}}. \tag{11}$$

According to the control loop in Fig. 7, current i_{q_ref} can be determined by $k_{vI}(v_{p\_\mathrm{ref}} - v_p)/s$. It can be represented as

$$\begin{aligned} i_{q\_\mathrm{ref}} &= \int_0^t -k_{vI}(V_p - v_{p\_\mathrm{ref}})e^{-\omega L k_{vI} t}dt \\ &= \frac{V_p - v_{p\_\mathrm{ref}}}{\omega L}e^{-\omega L k_{vI} t} - \frac{V_p - v_{p\_\mathrm{ref}}}{\omega L}. \end{aligned} \tag{12}$$

Due to the saturation block in Fig. 7, i_q can fall into one of the following three conditions:

(1) If $i_{q\_\mathrm{ref}} = |i_{q\,\lim}|$, solve (12). The obtained t is substituted into (11) to obtain $v_p(t) = \omega L{*}\,|i_{q\,\lim}| + V_p$.
(2) If $i_{q\_\mathrm{ref}} = -\,|i_{q\,\lim}|$, solve (12). The obtained t is substituted into (11) to obtain $v_p(t) = -\omega L{*}\,|i_{q\,\lim}| + V_p$.
(3) If $-\,|i_{q\,\lim}| < i_{q\_\mathrm{ref}} < |i_{q\,\lim}|$, v_p will be controlled at the reference value v_{p_ref}, i.e., $v_p(t) = v_{p\_\mathrm{ref}}$.

C. Calculation of Apparent Impedance Viewed By Relay Using Zbus Method and Comparison With Its Zone 2 Setting

The new PCC voltages obtained in (11) in Section III-B are used to calculate voltages at buses m and n based on the Zbus method. The obtained voltages include the effect of GSVSC control during fault k. They are given by

$$v_m = V_m - \sum_{p \in L} \frac{Z_{mp}}{Z_{pp}} v_p \tag{13}$$

$$v_n = V_n - \sum_{p \in L} \frac{Z_{np}}{Z_{pp}} v_p \tag{14}$$

where $Z_{m(n)p}$ is the transfer impedance between bus m(n) and bus p, Z_{pp} the driving point impedance corresponding to bus p, $V_{m(n)}$ is the voltage of bus m(n) during fault k, which can be obtained by the Zbus method discussed in Section III-A.

It is obtained that the voltage and current viewed by relay S are v_m and $(v_m - v_n)/Z_{m-n}$, respectively, where Z_{m-n} is the impedance of line m-n. The apparent impedance viewed by relay S can be represented as

$$Z_S = \frac{v_m}{(v_m - v_n) Z_{m-n}}. \tag{15}$$

The obtained impedance is compared with the Zone 2 setting of relay S for its operation evaluation. If the apparent impedance exceeds the Zone 2 setting, Zone 2 of relay S under-reaches its intended protection range.

IV. System Studies

The offshore wind HVDC network presented in Section II is connected to the IEEE 39-bus system for the analysis of miscoordinated distance relays. As shown in Fig. 8, GSVSC1 and GSVSC2 are connected to bus 29 and bus 23, respectively. The proposed combined ac/dc system is modeled in DIgSILENT PowerFactory. Each offshore wind farm is composed of 100 standard DFIGs, each rated at 5 MW. The bipolar VSC-HVDC link consists of four 600 MV, $\pm 150/132$kV VSCs. Control parameters of HVDC are shown in the Appendix. The commutating reactance of each VSC is 35 mH and the dc capacitor used to connect the positive pole and negative pole in the dc grid is 160 μm. Ten XLPE dc cables are used to construct the dc grid for the transmission of offshore wind power.

The IEEE 39-bus system is a 345 kV, 60 Hz ac grid, including 34 ac transmission lines with a nominal voltage equal to 345 kV, and a rating of 1.5 kA. Two ends of all transmission lines are equipped with distance relays. Zone 2 protection is set to reach 50% of the shortest line emanating from the remote bus with the time delay 0.37 s.

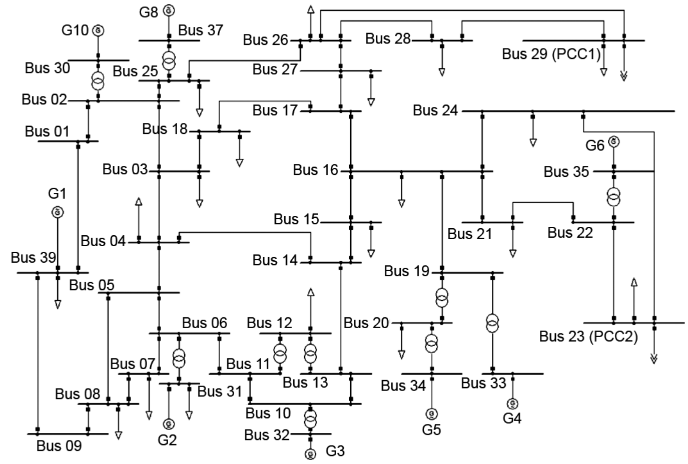

Fig. 8. IEEE 39-bus system.

A. Zone 2 Settings of Distance Relays

Two synchronous generators are connected to PCC1 and PCC2 to replace offshore wind HVDC network, respectively. The scenario of the modified ac grid is adjusted to ensure that the ac system will have identical power flow results with the combined ac/dc system. During an identical SC fault, the two systems have an identical initial state. Since the excitation system of synchronous generators (in the order of seconds) is a much slower voltage control compared with that of the VSC-HVDC, the comparison between the two models will clearly demonstrate the impact of the VSC-HVDC control.

The modified ac grid with synchronous generators is used to identify the Zone 2 settings of distance relays on the IEEE 39-bus system by fault simulations in DIgSILENT PowerFactory. A three-phase SC fault at the Zone 2 reach of a distance relay is initiated at 0 s on the modified ac grid. At the Zone 2 fault clearing time, i.e., 0.37 s, the impedance viewed by the relay is set as the Zone 2 setting of the corresponding relay on the IEEE 39-bus system with offshore wind HVDC network. By the fault simulation method, the Zone 2 settings of all distance relays on the combined ac/dc system are individually identified.

B. Calculation of Apparent Impedance Viewed by Distance Relays by Proposed Method

The proposed apparent impedance calculation method is applied to distance relays on the IEEE 39-bus system with offshore wind HVDC network. The impedance viewed by a distance relay on the combined ac/dc at the Zone 2 fault clearing time is calculated during a three-phase SC fault at its Zone 2 reach. The calculation results are compared with their corresponding Zone 2 settings obtained in Section IV-A. Since the phase angle of the calculated apparent impedance is close to that of the corresponding Zone 2 setting, the comparison between the calculated apparent impedance and Zone 2 setting is focused on the impedance magnitude. The results are shown in Table I. The calculated impedances of all listed relays have a deviation over 5% of their corresponding Zone 2 settings.

It is shown in Table I that the calculated impedances viewed by all listed relays exceed their corresponding Zone 2 settings. It is shown in Fig. 9 that eight of listed relays are on the remote

TABLE I
COMPARISONS BETWEEN CALCULATED IMPEDANCES VIEWED BY DISTANCE RELAYS ON COMBINED AC/DC GRID AT ZONE 2 FAULT CLEARING TIME AND ZONE 2 SETTINGS OF CORRESPONDING RELAYS

Relay	Calculated impedance (Ohm)	Zone 2 setting (Ohm)	Difference (over ±5%)
1 line 1-39	$198.00\angle 75.99^\circ$	$163.31\angle 79.98^\circ$	21.4%
2 line 2-25	$22.75\angle 65.83^\circ$	$19.61\angle 70.62^\circ$	16.0%
5 line 5-6	$8.82\angle 101.10^\circ$	$6.92\angle 105.32^\circ$	27.4%
7 line 6-7	$20.76\angle 93.71^\circ$	$17.25\angle 96.14^\circ$	20.3%
9 line 9-39	$318.54\angle 79.64^\circ$	$267.85\angle 79.75^\circ$	18.9%
11 line 6-11	$15.48\angle 84.19^\circ$	$14.29\angle 83.65^\circ$	8.3%
13 line 10-13	$6.92\angle 84.80^\circ$	$6.52\angle 93.00^\circ$	6.1%
17 line 16-17	$21.01\angle 90.00^\circ$	$19.04\angle 97.58^\circ$	10.3%
21 line 21-22	$33.83\angle 86.99^\circ$	$28.96\angle 109.42^\circ$	16.8%
22 line 22-23	$62.49\angle 92.89^\circ$	$58.21\angle 94.98^\circ$	7.4%
24 line 16-24	$40.09\angle 61.05^\circ$	$31.11\angle 46.09^\circ$	28.8%
24 line 23-24	$57.78\angle 92.55^\circ$	$50.95\angle 96.09^\circ$	11.8%
26 line 26-29	$87.15\angle 90.27^\circ$	$81.82\angle 89.30^\circ$	6.5%
27 line 26-27	$50.12\angle 87.35^\circ$	$47.73\angle 94.21^\circ$	5.0%
28 line 26-28	$278.60\angle 9.59^\circ$	$118.85\angle 13.69^\circ$	134.5%
28 line 28-29	$56.82\angle 101.87^\circ$	$41.86\angle 124.44^\circ$	64.3%
29 line 26-29	$211.14\angle 37.90^\circ$	$122.24\angle 38.60^\circ$	72.7%

Distance relay: i line i-j means bus i side relay on line i-j, and j line i-j means bus j side relay on line i-j.

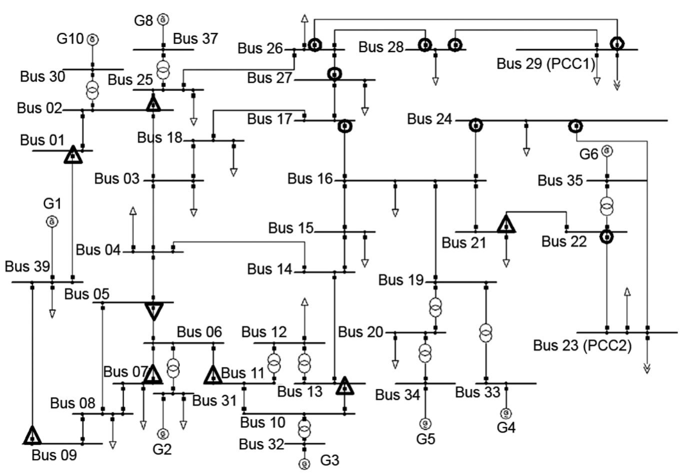

Fig. 9. Listed relays on IEEE 39-bus system.

ends of generator adjacent lines. They are marked by triangles while the other relays are marked by circles, as shown in Fig. 9.

An example is shown in Fig. 10 to analyze the marked relay by triangles on the remote end of generator adjacent lines. Relay A is located on the remote end of the adjacent line p-q of generator G. For the proposed apparent impedance calculation method, when line q-w experiences a three-phase SC fault F at 50% mid-line location, the calculated apparent impedance viewed by relay A is given by

$$Z_A = \frac{v_p}{\frac{(v_p - v_q)}{Z_{p-q}}} \tag{16}$$

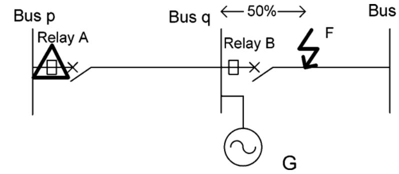

Fig. 10. Case of relay on remote end of generator adjacent line.

where v_p and v_q are the calculated nodal voltages, respectively; and Z_{p-q} is the impedance of line $p-q$.

As discussed in Section III-A, the transient impedances of generators are used to construct Zbus for the estimation of PCC voltages. The calculated nodal voltages correspond to the initial values of nodal voltages at the transient state. According to the decay pattern of the generator stator current during a SC fault on the generator adjacent line [6], it can be found that the stator current at the initial time of the transient state is larger than that at Zone 2 fault clearing time 0.37 s. As reported in Section IV-A, the Zone 2 setting of a relay is determined by the impedance viewed by the relay at the Zone 2 fault clearing time. The higher injection current between the fault point and relay location causes the impedance viewed by relay A at the initial time of the transient state to increase beyond its Zone 2 setting.

In the analysis of the impact of offshore wind HVDC network on distance relays, cases on the remote end of the generator adjacent line are separated. Therefore, relays in Table I marked by triangles are not included in the following analysis.

The remaining relays marked by circles are shown in Fig. 11. According to the analysis shown in Table I, the calculated impedances viewed by marked relays in Fig. 11 exceed their corresponding Zone 2 settings. It is found that Zone 2 protections of these relays under-reach due to the impact of offshore wind HVDC network. The deviation between the calculated impedance and Zone 2 setting reflects the extent of the impact of offshore wind HVDC network on distance relays. Relays with the larger deviation have a shorter Zone 2 reach. According to the location of these miscoordinated relays in Fig. 11, the level of the impact of offshore wind HVDC network on distance relays on the IEEE 39-bus system can be identified. The corresponding boundary is marked by a solid line, as shown in Fig. 11.

C. Boundary Verification Based on DigSILENT Simulations

A simulation method is used here to validate the analysis performed by the proposed method. To this end, the same ac/dc system with offshore wind HVDC network injections is modeled in DIgSILENT PowerFactory: three-phase SC faults at the Zone 2 reach of distance relays are individually simulated in the simulated combined ac/dc system to identify the impedance viewed by the corresponding relays at the Zone 2 fault clearing time. The obtained impedances are compared with the corresponding Zone 2 settings for the identification of miscoordinated relays. Relays with a deviation over 5% of their Zone 2 settings are listed in Table II.

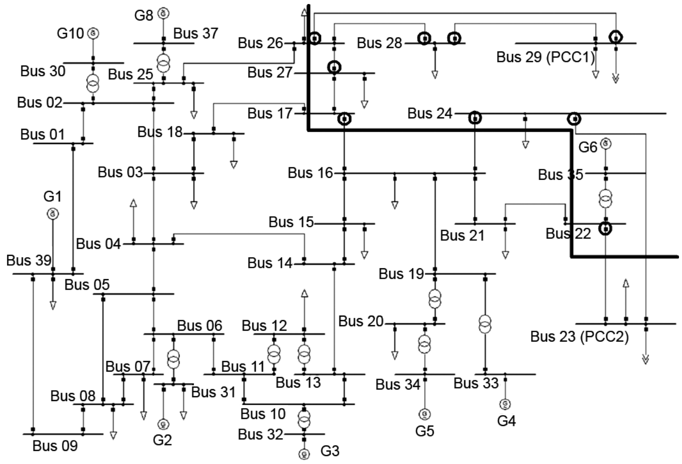

Fig. 11. Boundary of impact of offshore wind HVDC network on distance relays on IEEE 39-bus system based on proposed method.

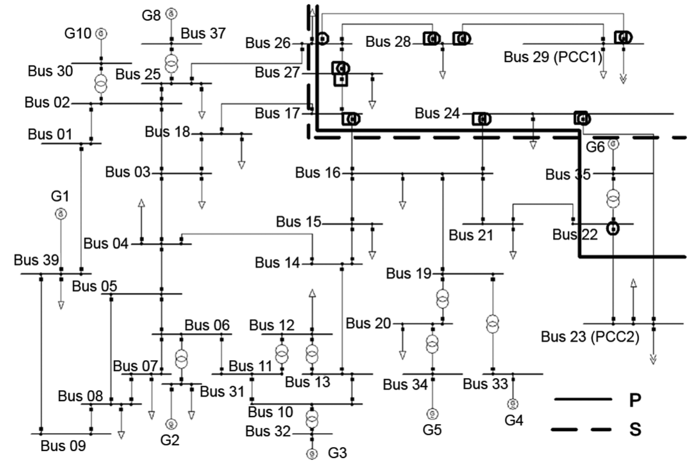

Fig. 12. Results comparison between proposed method and DIgSILENT simulation.

TABLE II
COMPARISONS BETWEEN IMPEDANCES VIEWED BY DISTANCE RELAYS ON COMBINED AC/DC SYSTEM AT ZONE 2 FAULT CLEARING TIME AND ZONE 2 SETTINGS OF CORRESPONDING RELAYS

Relay	Viewed impedance (Ohm)	Zone 2 setting (Ohm)	Difference (Over ±5%)
17 line 16-17	$20.00\angle 96.96^\circ$	$19.04\angle 97.58^\circ$	5.0%
24 line 16-24	$38.10\angle 46.11^\circ$	$31.11\angle 46.09^\circ$	22.4%
24 line 23-24	$56.63\angle 92.09^\circ$	$50.95\angle 96.09^\circ$	11.1%
27 line 17-27	$27.51\angle 84.12^\circ$	$26.10\angle 84.40^\circ$	5.4%
27 line 26-27	$51.60\angle 94.14^\circ$	$47.73\angle 94.21^\circ$	8.1%
28 line 26-28	$251.78\angle 12.76^\circ$	$118.85\angle 13.69^\circ$	111.2%
28 line 28-29	$57.19\angle 109.99^\circ$	$41.86\angle 124.44^\circ$	36.6%
29 line 26-29	$198.25\angle 84.40^\circ$	$122.24\angle 38.6^\circ$	62.2%

Distance relay: i line i-j means bus i side relay on line i-j, and j line i-j means bus j side relay on line i-j.

As shown in Table II, the apparent impedances viewed by the listed relays exceed the corresponding Zone 2 settings. It leads to the fault distance being overestimated in case of a three-phase SC fault experienced in the range of Zone 2. These miscoordinated relays are marked by squares in Fig. 12. The corresponding boundary referred to the impact level of offshore wind HVDC network is highlighted by a dashed line, as shown in Fig. 12.

The results using the proposed method in Section IV-B are also shown in Fig. 12, i.e., relays marked by circles. By comparison of the results obtained by two methods, the nonoverlapping relays include bus 22 side relay on line 22–23, bus 26 side relay on 26 line 26–29 and bus 27 side relay on line 17–27. Their results using both methods are shown in Table III.

It is shown in Table III that all three relays show higher apparent impedances than the corresponding Zone 2 settings by both of methods. They are not shown as matched in Fig. 12 due to the pre-set deviation level of 5%. Further analysis in Table III indicates that the proposed method accurately identifies miscoordinated relays and the level of the impact of offshore wind HVDC network on distance relays.

TABLE III
RESULTS OF NONOVERLAPPING RELAYS BY PROPOSED METHOD AND FAULT SIMULATION IN DIGSILENT POWERFACTORY

Relay	Calculated impedance by P (Ohm)	Viewed impedance by S (Ohm)	Zone 2 setting (Ohm)	Difference	
				P	S
22 line 22-23	$62.49\angle 92.89^\circ$	$60.72\angle 89.21^\circ$	$58.21\angle 94.98^\circ$	7.4%	4.3%
26 line 26-29	$85.2\angle 89.02^\circ$	$87.15\angle 90.27^\circ$	$81.82\angle 89.30^\circ$	6.5%	4.1%
27 line 17-27	$26.89\angle 84.17^\circ$	$27.51\angle 84.12^\circ$	$26.10\angle 84.40^\circ$	3.0%	5.4%

Distance relay: i line i-j means bus i side relay on line i-j, and j line i-j means bus j side relay on line i-j,
P: Proposed method; S: Simulation method by DIgSILENT PowerFactory.

D. Boundary Identification With Consideration of Actual Condition

In current power grids, many planned offshore wind farms are yet to be constructed and integrated into the onshore grids. It is useful to compare the scenarios with and without the offshore wind generations. To this end, Zone 2 settings of distance relays on the IEEE 39-bus system are identified without offshore wind HVDC network. Since the transmitted offshore wind power in the proposed offshore wind HVDC network is 1 GW, identical loads are reduced in the IEEE 39-bus system to balance its power flow, including 50 MW of load 03 (the load connected to bus 03), 100 MW of load 04, 50 MW of load 16, 50 MW of load 18, 100 MW of load 21, 150 MW of load 23, 100 MW of load 24, 100 MW of load 25, 50 MW of load 26, 250 MW of load 29. The obtained new ac grid G' is used to individually identify the new Zone 2 settings of the combined ac/dc system by performing fault simulations in DIgSILENT PowerFactory.

Neglecting relays on the remote end of generator adjacent lines, the calculated impedances viewed by distance relays on the combined ac/dc system are compared with the corresponding new Zone 2 settings. Since the new ac grid G' has different power flow from the IEEE 39-bus system with offshore wind power injection, the different nodal voltages are

TABLE IV
CONTROL PARAMETERS OF VSCs

Symbol of Control parameters	Value
k_{iP} (k_{iI})	2.98 (1/0.0273)
k_{vP} (k_{vI})	2 (1/0.07)
$i_{\lim}$ (Current limitation value of VSCs)	1.08 p.u.
$i_{q\lim}$	0.8 p.u.
T_m (τ_i)	0.01 s (0.002 s)
P_{ref} (active power setpoint of P-V droop)	250 MW
v_{dc_ref} (v_{p_ref})	1.01 p.u. (1.01 p.u.)
k (slope of P-V droop)	0.025 V/kW

likely to affect the impedances viewed by distance relays. It is difficult to judge whether the deviation between the calculated impedance and its Zone 2 setting is caused by offshore wind HVDC network. However, the calculated impedance viewed by relays marked by circles in Fig. 11 still perform higher values than the corresponding new Zone 2 settings.

V. CONCLUSION

When a transmission line close to PCCs experiences a three-phase SC fault in a combined ac/dc system, its backup protection relay tends to overestimate the fault distance due to reactive power control of VSC-HVDC. An accurate apparent impedance calculation method is proposed to identify miscoordinated distance relays in an ac grid with offshore wind HVDC network injections. The proposed method provides a quantitative measure of the level of impact of offshore wind HVDC network on distance relays. The corresponding boundary reflects the miscoordinated area in the ac grid with HVDC-connected offshore wind generators. With the growing penetration of offshore wind farms, a significant addition of VSC-HVDC links will be connected to the ac mainland grid. For the given HVDC parameters, the proposed method can be used to find the miscoordinated relays of an ac grid with offshore wind HVDC network that need to be adjusted.

APPENDIX

The control parameters of VSC are shown in Table IV.

ACKNOWLEDGMENT

The authors would like to thank Dr. J. Yan from Iowa State University for his contributions in the development of the IEEE 39-bus system model for dynamic simulations.

REFERENCES

[1] K. Bell, D. Cirio, A. M. Denis, L. He, C.-C. Liu, C. Moreira, and P. Panciatici, "Economic and technical criteria for designing future offshore HVDC grids," presented at the IEEE Power Energy Soc.: Innovative Smart Grid Technol, Gothenburg, Sweden, 2010.

[2] L. Xu, L. Yao, and C. Sasse, "Grid integration of large DFIG based wind farms using VSC transmission," *IEEE Trans. Power Syst.*, vol. 22, no. 3, pp. 976–984, Aug. 2007.

[3] W. Lu and B. T. Ooi, "Optimal acquisition and aggregation of offshore wind power by multiterminal voltage-source HVDC," *IEEE Trans. Power Del.*, vol. 18, no. 1, pp. 201–206, Jan. 2003.

[4] L. He and C.-C. Liu, "Protection coordination between a HVDC offshore wind system and AC grid," in *Proc. CIGRE Symp. Elect. Power Syst. Future*, Bologna, Italy, Sep. 13–15, 2011.

[5] P. M. Anderson, *Power System protection*. New York: IEEE, 1999.

[6] P. Kundur, *Power System Stability and Control*. New York: McGraw-Hill, 1994.

[7] T. S. Sidhu, R. K. Varma, P. K. Gangadharan, F. A. Albasri, and G. R. Ortiz, "Performance of distance relays on shunt-FACTS compensated transmission lines," *IEEE Trans. Power Del.*, vol. 20, no. 3, pp. 1837–1845, Jul. 2005.

[8] X. Zhou, H. Wang, R. K. Aggarwal, and P. Beaumont, "Performance evaluation of a distance relay as applied to a transmission system with UPFC," *IEEE Trans. Power Del.*, vol. 20, no. 3, pp. 1237–1147, Jul. 2006.

[9] P. K. Dash, A. K. Pradhan, G. Panda, and A. C. Liew, "Adaptive relay setting for flexible AC transmission system (FACTS)," *IEEE Trans. Power Del.*, vol. 15, no. 1, pp. 38–43, Jan. 2000.

[10] A. K. Pradhan and G. Joos, "Adaptive distance relay setting for lines connecting wind farms," *IEEE Trans. Power Del.*, vol. 22, no. 1, pp. 206–213, Jan. 2007.

[11] T. S. Sidhu, D. S. Baltazar, R. M. Palomino, and M. S. Sachdev, "A new approach for calculating zone-2 setting of distance relays and its use in an adaptive protection system," *IEEE Trans. Power Del.*, vol. 19, no. 1, pp. 70–77, Jan.. 2004.

[12] N. Acharya and C.-C. Liu, "Tripping of wind turbines during a system fault," in *Proc. IEEE Power Energy Soc. Gen. Meeting*, Jul. 2008, pp. 1–8.

[13] Z. X. Han, "Generalized method of analysis of simulation faults in electric power system," *IEEE Trans. Power App. Syst.*, vol. PAS-101, no. 10, pp. 3393–3942, Oct. 1982.

[14] A. Yazdani and R. Iravani, "Voltage-sourced converters in power systems modeling," in *Control and Applications*. Hoboken, NJ, USA: Wiley, 2009.

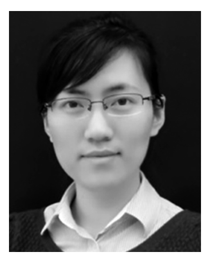

Lina He (S'11) received the B.S. and M.S. degrees in electrical engineering from Huazhong University of Science and Technology, Wuhan, China, in 2007 and 2009, respectively, and is currently pursuing the Ph.D. degree in electrical engineering at University College Dublin, Dublin, Ireland.

She was an Engineer at Tianjin Electric Power Corporation, State Grid Corporation of China, Tianjin, China, during 2009–2010. Her research interests include the protection and defense of the HVDC offshore wind networks, and wide-area voltage protection of smart grids.

Chen-Ching Liu (F'94) received the Ph.D. degree in electrical engineering from the University of California, Berkeley, CA, USA.

Currently, he is the Boeing Distinguished Professor at Washington State University, Pullman, WA, USA and Professor of Power Systems at University College Dublin, Dublin, Ireland. He was Palmer Chair Professor of Electrical Engineering at Iowa State University and a Professor of Electrical Engineering at the University of Washington.

Andrea Pitto (S'06–M'10) received the M.Sc. and Ph.D. degrees in electrical engineering from the University of Genoa, Genoa, Italy, in 2009 and 2010, respectively.

He was a Research Assistant at the Naval and Electrical Engineering Department, Genoa University, during 2009–2010. He joined Ricerca sul Sistema Energetico S.p.A (RSE) in 2011. His research interests include probabilistic and deterministic approaches to power system security assessment, simulation of cascading mechanisms in extremely high voltage grids, and modelling and control of HVDC transmission systems for offshore wind power integration.

Dr. Pitto is a member of the IEEE Task Force, "Understanding, Prediction, Mitigation and Restoration of Cascading Failures," of the IEEE Power and Energy Society Computer and Analytical Methods Subcommittee (CAMS).

Diego Cirio (SM'13) received the M.Sc. and Ph.D. degrees in electrical engineering from the University of Genoa, Genoa, Italy, in 1999 and 2003, respectively.

He was with CESI during 2003–2005, involved in consultancy activities for the Operations department of the Italian Transmission System Operator. Currently, he is with Ricerca sul Sistema Energetico-RSE S.p.A., where he leads the Grid and Infrastructure Security research group within the Power System Development Department. He is involved in national and EU research projects on power system security and probabilistic risk assessment and control. His research interests include power system security and operational risk assessment also with large penetration of wind power, wide-area monitoring and control, and restoration.